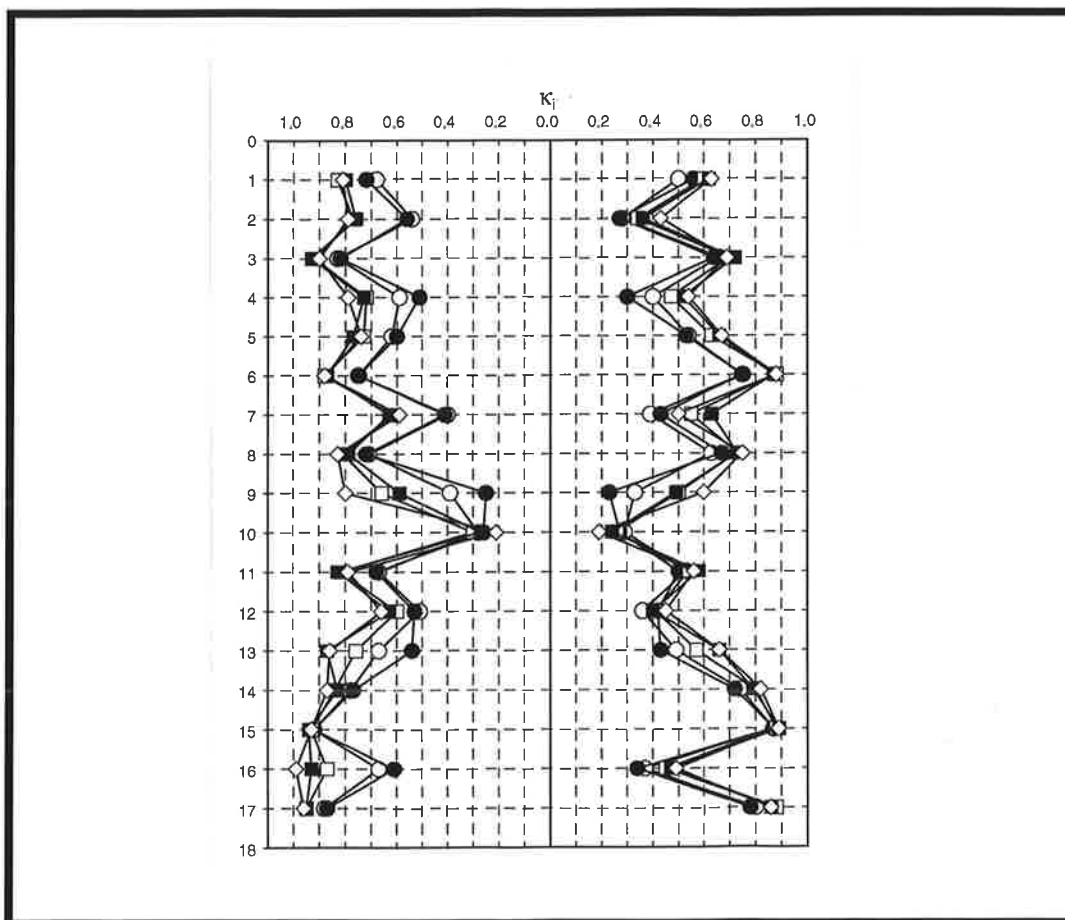




Max-Planck-Institut für Meteorologie

REPORT No. 131



ON COUPLING GLOBAL BIOME MODELS WITH CLIMATE MODELS

by

MARTIN CLAUSSEN

Hamburg, April 1994

AUTHOR:

Martin Claussen

Max-Planck-Institut
für Meteorologie

Max-Planck-Institut
für Meteorologie
Bundesstraße 55
D-20146 Hamburg
F.R. Germany.

Telephone:	from Germany:	international:
	(040) 41173-0	+49 40 41173-0
Telefax:	from Germany:	international:
	(040) 41173-298	+49 40 41173-298

E-Mail Adresse:

<name> @ dkrz.d400.de

On coupling global biome models with climate models

Martin Claussen

Max-Planck-Institut für Meteorologie

Bundesstr.55

20146 Hamburg, Fed. Rep. Germany

Abstract

The BIOME model of Prentice et al. (1992), which predicts global vegetation patterns in equilibrium with climate, is coupled with the ECHAM climate model of the Max-Planck-Institut für Meteorologie, Hamburg. It is found that incorporation of the BIOME model into ECHAM, regardless at which frequency, does not enhance the simulated climate variability, expressed in terms of differences between global vegetation patterns. Strongest changes are seen only between the initial biome distribution and the biome distribution computed after the first simulation period, provided that the climate-biome model is started from a biome distribution that resembles the present-day distribution. After the first simulation period, there is no significant shrinking, expanding, or shifting of biomes. Likewise, no trend is seen in global averages of land-surface parameters and climate variables.

Significant differences in the results of the climate-biome model are found when single-year and multi-year climatologies are compared regardless whether climate and biome model are used in an off-line mode or are interactively integrated. It is concluded that a biome model should be coupled with a climate model in the following way: Firstly, the climate model should be integrated over several years; secondly, a biome distribution should be computed from the corresponding multi-year simulated climatology; finally, land-surface parameters are to be deduced from the biome distribution as boundary condition of the climate model for a subsequent integration, and so on until an equilibrium is established.

Starting the climate-biome model from a biome map which drastically differs from today's global distribution of biomes but keeping present-day ocean temperatures fixed, it takes several iterations until the model finds its new equilibrium which differs from the present-day vegetation distribution in certain parts of the globe. This study indicates that the South-West part of the Sahara and the Indian subcontinent are sensitive to vegetation changes which go in line with a weakening of the Azores high pressure system and a deterioration of the Indian summer monsoon.

1 Introduction

The climate system consists of several subsystem which interact in a complex, nonlinear way at a wide range of time scales. Although the sensitivity of climate simulations to changes in vegetation patterns is well documented (e.g. Mintz, 1984), little attention has been paid to the interactive integration of biosphere and atmosphere. By contrast, the interaction between other components of the climate system, mainly atmosphere and ocean, has quite intensively been studied during the last few years (e.g. Cubasch et al., 1992). So far, global vegetation schemes have been used to compute global vegetation patterns and even potential vegetation shift due to a possible greenhouse gas induced climate warming from climate simulations in a diagnostic (or one-way) mode (e.g. Prentice and Fung, 1990, Monserud and Leemans, 1992, Monserud et al., 1993, Claussen and Esch, 1994)

Perhaps the first and so far the only attempt to incorporate continental vegetation as a dynamic component of a global climate model has been undertaken by Henderson-Sellers (1993). In her study, a simplified Holdridge scheme is used which is an static, diagnostic vegetation model. As an important result, Henderson-Sellers finds the vegetation scheme to be a stable component of the global climate system without any discernable trends being observed over the integration period. Differences between simulations with and without interactive vegetation turned out to be rather small. Unfortunately, the interactive integration was carried out over a rather short period of 5.6 years due to hardware problems. Hence Henderson-Sellers did not study the problem of coupling vegetation with climate models in great detail. Therefore, the technical problems of integrating a combined climate-vegetation model will be addressed in this paper.

In Section 2, the two components of the interactive model, a general circulation model of the atmosphere and a vegetation prediction scheme as biospheric component, are briefly presented. Since there exist at present no global dynamic vegetation models, the biospheric component consists of a biome model which predicts vegetation zones (or, equivalently, biomes) which are in equilibrium with climate. In Section 3, the method of combining climate and biome model is discussed.

The central purpose of this study is to explore the consequences of varying the frequency of asynchronous coupling a climate model with a biome model and to analyse the way

the model finds its own equilibrium. Therefore, in a first experiment, described in Section 4, the climate-biome model is initialized with a global biome distribution which resembles that of present-day climate. Several integrations are performed to analyse the effects of varying frequency of coupling the atmospheric with the biospheric component on variability and trends of global vegetation patterns, land-surface parameters, and climate variables.

Using the experience gained in the first experiment, a second experiment, discussed in Section 5, is set up starting from a global biome pattern which drastically differs from today's distribution. This experiment should indicate how sensitive the climate-biome model is to initial disturbances and whether it finds a new equilibrium state. This problem is associated with the question in which parts of the globe vegetation changes remain stable. However, the reader is asked not to overinterpret the results of this study. It is a study of processes rather than an exercise of predicting realistic global vegetation patterns. It should, nevertheless, provide guidance in designing such exercise.

2 Climate model and biome model

2.1 The climate model

As atmospheric component of the combined climate-biome model, the climate model ECHAM, developed at the Max-Planck-Institut für Meteorologie in Hamburg, is taken. The model physics as well as its validation is described in detail by Roeckner et al. (1992).

In the original version of ECHAM (level 3), there are no specific biomes or vegetation types prescribed. Instead, a vegetation ratio is assigned to each grid box using data of Wilson and Henderson-Sellers (1985), a background albedo (albedo of snow-free land surfaces) is derived from satellite data of Geleyn and Preuss (1983), and roughness length is computed from the variance of orography (Tibaldi and Geleyn, 1981) and from a vegetation roughness length given by Baumgartner et al. (1977). Also a forest ratio (in analogy to vegetation ratio) from Matthews' (1984) data is prescribed which

is used to compute the albedo of snow-covered forested areas. The leaf area index and minimum stomatal resistance are global constants. Despite these rather crude representation of vegetation in ECHAM, the global patterns of biomes computed from ECHAM climatology agree quite well with those computed from the IIASA (International Institute of Applied Systems Analysis) climate data (Claussen and Esch, 1994) by using the BIOME model of Prentice et al.(1992).

To allow for coupling with a vegetation model, ECHAM was modified such that arbitrary global data of background albedo, roughness length, vegetation ratio, leaf area index, and forest ratio can be specified.

2.2 The biome model

Biomes are computed by using the BIOME model of Prentice et al. (1992). Prentice's et al. (1992) model is chosen, because this model is based on physiological considerations rather than on correlations between climate distribution and biomes as they exist today. Biomes are not taken as given as, for instance, in the Holdrige classification, but emerge through the interaction of constituent plants. Hence the biome model can be applied to the assessment of changes in natural vegetation patterns in response to different climate states. However, it is important to notice that the BIOME model does not simulate the transient dynamics of vegetation. At best, it provides constraints within which plant community dynamics should operate.

In the BIOME model, 14 plant functional types are assigned climate tolerances in terms of amplitude and seasonality of climate variables. The cold tolerance of plants is expressed in terms of a minimum mean temperature of the coldest month. Some plant types also have chilling requirements expressed in terms of a maximum mean temperature of the coldest month.

The heat requirement of plant types is given in terms of annual accumulated temperatures over 5°C, for some plant types a threshold of 0°C is used. The heat requirement of some shrub types is given by the mean temperature of the warmest month.

The third basic climate tolerance is associated with moisture requirement in terms of

annual moisture availability. All plant types, except for desert shrub, have minimum tolerable values of annual moisture availability. Only tropical rainforest also has a maximum tolerable value. The annual moisture availability is defined as ratio of actual evapotranspiration (AET) and potential evapotranspiration (PET). PET basically depends on net-radiation, i.e. solar radiative input, radiative cooling, and cloudiness. AET, in addition, requires prescription of precipitation and soil water capacity. Hence for evaluation of annual moisture availability, monthly means of temperature, precipitation, cloudiness, and information on soil water capacity are needed as input variables. (Actually the BIOME model uses sunshine in terms of percentages of possible hours of bright sunshine, i.e. an inverse measure of cloudiness.)

The BIOME model predicts which plant functional type can occur in a given environment, i.e. in a given set of climate variables. Then the BIOME model selects the potentially dominant plant types according to a dominance hierarchy. Finally, biomes are defined as combinations of dominant types. The dominance hierarchy is an artificial device whose main purpose is to facilitate comparison with the global vegetation classification of Olson et al. (1983).

Prentice et al. (1992) have used the IIASA climate data base, described by Leemans and Cramer (1990), and soil texture data (to estimate soil water capacity) from the FAO soils map (FAO, 1974). Their predictions of global patterns of biomes are in fair agreement with the global distribution of actual ecosystem complexes being evaluated by Olson et al. (1983). Where intensive agriculture has obliterated the natural vegetation, comparison of predicted biomes and observed ecosystems is, of course, omitted.

3 Coupling climate model with biome model

The coupling of ECHAM with the BIOME model is done in a rather simple way. ECHAM produces monthly means of near-surface temperature, precipitation, and cloudiness. From these data, the BIOME model evaluates climate constraints mentioned in the previous Section 2.2 and, subsequently, a global distribution of biomes using the

same grid as the climate model. From the biome map, a global set of surface parameters, i.e. background albedo α , roughness length z_0 , vegetation ratio c_v , leaf area index LAI , and forest ratio c_F , needed in ECHAM, are deduced. With this new set of surface parameters a subsequent integration with ECHAM is performed. The problems are: at which frequency should this iteration be done, and how are the surface parameters allocated to biomes?

3.1 Allocation of surface parameters

Allocation of surface parameters to biomes is done in the following way. Firstly, an albedo α_v and roughness length z_{0v} of vegetation are allocated to Olson's et al. (1983) major ecosystem complexes basically following Henderson-Sellers et al. (1986) (for details see Claussen *et al.*, 1994). The forest ratio of each ecosystem complex is a rough first guess from Olson's et al. description of forest and woodland structure. Leaf area index and vegetation ratio are prescribed following Lieth and Essers suggestions (cited in Heise *et al.*, 1988). Allocation of LAI to ecosystem complexes is certainly a problem since they are poorly correlated (Esser, personal communication). It seems more reasonable to infer LAI from data of net primary production (npp) of vegetation. However, allocation of plant types to npp is still in progress as a new version of the BIOME model is being developed (Prentice, personal communication). Hence, for the time being, LAI and c_v are taken as a first guess which is sufficient for this study which just explores the consequences of coupling a biome model with a climate model, but does not pretend to predict realistic global vegetation patterns.

Secondly, Olson's et al. ecosystem complexes are allocated to Prentice's et al. biomes (for details the reader is referred to Table 4 in Prentice et al., 1992). This is done by averaging surface parameters of ecosystem complexes (weighted with its relative coverage of continental surfaces) to obtain surface parameters for each biome. (Only z_{0v} is not directly averaged, but computed from an average of drag coefficients taken at a blending height of 100m, see Claussen, 1991.) The final values are given in Table 1.

	Biome name	α_v	LAI	c_v	c_F	$z_{0v}(m)$
01	tropical rain forest	0.12	9.3	0.96	1.0	2.000
02	tropical seasonal forest	0.12	4.8	0.81	0.9	2.000
03	savanna	0.15	2.9	0.60	0.6	0.361
04	warm mixed forest	0.15	6.6	0.83	0.8	0.716
05	temperate deciduous forest	0.16	3.5	0.59	1.0	1.000
06	cool mixed forest	0.15	2.6	0.51	1.0	1.000
07	cool conifer forest	0.13	9.1	0.96	1.0	1.000
08	taiga	0.14	4.1	0.68	0.9	0.634
09	cold mixed forest	0.15	2.6	0.51	1.0	1.000
10	cold deciduous forest	0.14	4.1	0.68	0.9	0.634
11	xerophytic woods / shrub	0.18	3.2	0.60	0.2	0.111
12	warm grass / shrub	0.20	1.0	0.29	0.0	0.100
13	cool grass / shrub	0.19	1.3	0.34	0.0	0.055
14	tundra	0.17	1.5	0.39	0.1	0.033
15	hot desert	0.28	0.3	0.08	0.0	0.004
16	cool desert	0.28	0.3	0.10	0.0	0.005
17	ice / polar desert	0.15	0.0	0.00	0.0	0.001

Table 1: Allocation of surface parameters used in the climate model to biomes specified in Prentice et al. (1992) BIOME model.

Finally, the roughness length z_0 is computed from z_{0v} by

$$z_0 = (z_{oro}^2 + z_{0v}^2)^{1/2} \quad (1)$$

according to the specification of roughness in ECHAM. z_{oro} is the roughness length associated with form drag due to subgrid-scale orography exerted on atmospheric flow. In mountainous areas, z_0 changes little with vegetation since, there, z_{oro} is much larger than z_{0v} . The background (surface) albedo α is assumed to be given as

$$\alpha = c_v \alpha_v + (1 - c_v) \alpha_s \quad (2)$$

where α_s is the albedo of bare soil. α_s is taken from ERBE satellite data (Claussen et al., 1994) and assumed to be constant during the iterative coupling of ECHAM with BIOME model. This assumption implies a rather moderate global influence of changes in vegetation to background albedo, since, in this study, $c_v \sim 0.5$ on global average. Moreover, it is questionable whether soil properties remain unaffected by

changes in vegetation. Therefore, to explore the consequences of a more direct coupling of background albedo to vegetation, $\alpha = \alpha_v$ in a second experiment with the exception that $\alpha = 0.35$ is specified for biomes 15 and 16, hot desert and cool desert, to take into account that bare sand deserts may have albedos larger than sparsely vegetated deserts. (For instance, in the Sahara, an albedo of up to 0.4 is observed).

3.2 Setup of experiments

In her experiment, Henderson-Sellers (1993) calculated a new vegetation distribution and incorporated it into the climate model at the end of each 12 month period. Such a relatively short period was justified by arguing that the year-to-year variability of all vegetation changes computed in an off-line mode is rather small, roughly 10% of the continental surface. Claussen (1993) investigated the shift of biomes due to simulated climate variability. He used the BIOME model of Prentice et al. (1992) to estimate global vegetation patterns from climatologies simulated by the climate model ECHAM and he found larger numbers of some 30% difference when comparing biomes evaluated from a single-year simulation and a 10-year simulation. Hence either the BIOME model is more sensitive to climate variation than the Holdrige scheme, or ECHAM produces larger interannual variance than the NCAR CCM climate model used by Henderson-Sellers. In any case, it seems worthwhile to explore the consequences of letting the biome model and the climate model interfere at various frequencies. Since the BIOME model is a static model and since the combined climate-biome model can just be used to let the system integrate into an equilibrium state, a migration criterion as proposed by Martin (1993) for the coupling of dynamic vegetation models with climate models, a criterion which determines the ratio of spatial and temporal incrementation of both models, can be ignored.

In a first experiment, four series of integrations are set up. Firstly, climate model and biome model are run in an off-line mode for 10 years, called run A, and the (virtual) interannual variability of biome patterns and associated (virtual) change of land surface parameters is evaluated. Averaging over the first and the last five years, differences of biome patterns computed from single-year and 5-year climatologies are estimated. In a second 10-year run, called run B, biomes and, subsequently, surface parameters are

computed and incorporated into the climate model at the end of each year, i.e. in an on-line or two-way interactive mode. In a third 20-year run, called run C, the exchange of information between submodels is done every five years. Hence biomes are estimated from simulated climate data averaged over five years. In the fourth run, called run D, the same is done, but for a 10-year period. The last run was stopped after 20 years of integration.

The first experiment is started from a global distribution of biomes which closely resembles the present-day biome patterns shown in Prentice et al. (1992). In a second experiment, a drastic change in vegetation patterns is initially prescribed: all desert is replaced by tropical rain forest and all rain forest, tropical seasonal forest, and savanna, by desert. In a 22-year integration, an equilibrium between climate and vegetation is sought to be established. Climate model and biome model are coupled at a frequency of initially six and subsequently four years as a result of the first experiment which will be outlined in the following section.

4 Testing the frequency of coupling

As mentioned in the previous section, the first experiment consists of four integrations (run A, B, C, D) which differ by the frequency at which information between climate and biome model is exchanged. These four integrations are analysed in terms of trends and differences between global surface parameters, climate constraints, interannual variability of biome patterns, and structure of biome patterns.

4.1 Variability of biome patterns

Figure 1 depicts the interannual differences Δ of biomes distributions. Δ is defined as the total area, in term of percentage land surface, Antarctica excluded, in which biomes differ when comparing two global biome distributions. (For example, the point between abscissa labels 0 and 1 indicates that for almost 35% of the continental surface, Antarctica excluded, biomes of the distribution evaluated at the end of the first 12-

year period and of the initial biome distribution are different.) The full line indicates differences between biome patterns computed from climate simulations in an off-line mode, run A, the dashed line refers to results from the coupled climate-biome model in run B.

From Figure 1, it is obvious that the largest change is seen between the initial biome distribution and the biome distribution computed after the first period of climate integration, in the following referred to as the first iteration. After the first year, interannual differences do not exhibit a significant trend, neither for the off-line nor the on-line mode. Excluding the first iteration, the average interannual difference amounts to 27.1% and 25.7% in the off-line and on-line mode, respectively. When applying a student's t-test, it is seen that there is no significant difference between these average values.

Figure 2 is the same as Figure 1, except that differences Δ between successive 5-year integrations are shown (run C). As also seen in Figure 1, the largest change (here, 27.5%) occurs at the first iteration. Subsequent differences are smaller (here, 13.35% on average). In contrast to run A and B, run C exhibits a significant trend (at 5% significance level), but this trend is quite small (less than 7% land area per 5 years). When biomes are computed from first and the last 5 years of the off-line mode run A and of the on-line mode run B, it is found that differences between successive 5-year climatologies amount to 13.39% and 13.07%, respectively. Moreover, when comparing all combinations of 5-year climatologies, differences randomly vary in between 12.5% - 15.8%. Hence it can be concluded that differences between biomes distributions from various 5-year integrations are insignificant, regardless whether computation is done in an off-line mode or different on-line modes.

Not shown here as a Figure are results from the 20-year integration run D in which biomes have been computed from the first and the last 10 years and where new surface parameters are incorporated into the climate model after the first 10 years. The difference Δ between the initial biome distribution and that computed from the climatology of the first 10 years amounts to 25.8%, and that between biomes from the first and the second 10 years, 12.6%. Moreover, when comparing the latter biome distribution with the distribution computed from a 10-year average over results of run B, then differences of 12.0% and 12.6% are found. These numbers are within (albeit at the upper limit of)

the 9% - 12% range which Claussen (1993) found by comparing various biome distributions computed from various 10-year integrations with ECHAM both at T21 and T42 resolution, all done in an off-line mode.

In summary, it can safely be stated that incorporation of the BIOME model into the climate model ECHAM does not enhance the simulated variability, expressed in terms of differences between distributions of vegetation or, equivalently, climate zones. Moreover, the frequency at which the biome and the climate model interfere does not significantly alter the degree of interannual, pentadal, or decadal variability.

4.2 Global agreement of biome patterns

The structure of global biome patterns of run A, B, C, D is analysed using Kappa statistics. The Kappa statistics is presented by Monserud and Leemans (1992) as an objective tool for comparing global vegetation maps. Such maps can result from either compilations of observed spatial patterns or from simulations from models that are global in scope. Monserud and Leemans (1992) illustrate this method by comparing global maps resulting from applying a modified Holdridge Life Zone classification to current climate and several climate change scenarios. Prentice et al. (1992) used a modified version of the original Kappa statistics to evaluate the performance of their BIOME model. Here, the original Kappa statistics as outlined by Monserud and Leemans (1992) in detail is applied to explore the similarity of vegetation maps obtained from run A, B, C, and D. In contrast to the analysis of land coverage as done in the previous section 4.1, Kappa statistics also indicates, if biomes are just shifted without changing their total area occupied. In the latter case, Kappa statistics would indicate poor agreement, whereas the analysis of the previous section would yield no difference.

For details of the Kappa statistics, the reader is referred to Monserud and Leemans' (1992) paper. Here, it should be sufficient to mention that there are two Kappa values, a κ which indicates global or overall agreement between two maps and a vector κ_i which is a measure of agreement considering a specific biome (number i). Monserud and Leemans (1992) proposed the following threshold values for separating the different degrees of agreement for the Kappa statistics which are listed in the following table:

Lower bound	Degree of agreement	Upper bound
<0.05	no	0.05
0.05	very poor	0.20
0.20	poor	0.40
0.40	fair	0.55
0.55	good	0.70
0.70	very good	0.85
0.85	excellent	0.99
0.99	perfect	1.00

In Figure 3a, b, the global Kappa values of run A and B are presented. Full and open diamonds (Figure 3a) indicate agreement of biomes maps between two successive years of run A and run B, respectively. It appears that the agreement between the initial biome map and the biome map computed after the first year of integration is good, $\kappa = 0.62$. After the first year, there is no trend, and, on average, $\kappa = 0.70$ for run A and $\kappa = 0.72$ for run B. These average values do not differ significantly.

In Figure 3b, the curves labeled with full and open squares indicate agreement of the initial biome pattern and the biome patterns computed at the end of each year of run A and run B, respectively. Obviously, there is no apparent trend, and run A and B both yield $\kappa = 0.62$ on average over the 10 years.

In Figure 3b, the curves labeled with full and open circles indicate global agreement of maps of run A and run B, respectively, with a biome map which has been produced from an earlier 30-year integration of the climate model ECHAM in its original version level 3 (see Claussen, 1993). This run is referred to as run 30 in the following. In run 30, the same sea surface temperature (SST) data are used as for the present run A, B, C, D. However, different land-surface parameters are taken as discussed in Section 4.5. It appears that biome patterns computed from run A and run B agree better with run 30 than with the initial biome distribution. Further analysis of data shown in Figure 3b reveals that there is no significant trend and no significant differences between Kappa values estimated from run A and run B.

Results of the analysis of run C and run D, which are not presented as Figures here, are the following. It is found that comparison of all biome maps computed from run C and run D yield Kappa values just below $\kappa = 0.7$, i.e. biome maps from run C and

run D agree better with the initial biome map than biome maps from run A and run B. Comparison between biome maps of run C and run D with that of run 30 yields $0.82 < \kappa < 0.84$ which is, again, much better an agreement than of run A, B with run 30. As for run A and run B, there is no significant trend in Kappa values after the first iteration. (For run D, statistics has zero degrees of freedom.)

In summary, it appears that biome maps do not change significantly after the first iteration, regardless whether biomes are computed in an off-line or on-line mode with the climate model. Together with the result of the previous section 4.1, it can be concluded that, apart from a minor exception, there is no significant shrinking, expanding or shifting of biomes. Moreover, the climate-biome model finds its own equilibrium; the equilibrium biome distribution differs from the initial one and resembles more the original one (run 30).

4.3 Structure of biome patterns

In the previous Section 4.2, it has been found that there is a difference in global agreement of run A, B on the one side, and run C, D on the other side. Moreover, there is better agreement of run A, B, C, D with run 30 than with the initial biome distribution. To analyse this result in more detail, the agreement of individual biomes, i.e. the vector κ_i is studied.

Figure 4 depicts the agreement vector κ_i (for allocation of biome numbers to biome names see Table1). On the left-hand side of the figure, agreement with run 30 is plotted and on the right-hand side, agreement with the initial biome distribution. Values of κ_i are averaged over all maps of run A, B, C, D, respectively.

At the first glance, left-hand side and right-hand side of Figure 4 are similar, biomes showing better agreement with biomes of run 30 also exhibit better agreement with biomes of the initial map and vice versa. However, it is also seen why there is better agreement between maps of run A,B,C,D and run 30 than between run A,B,C,D and the initial biome map. When considering the five most wide spread biomes (which cover the largest portion of continents), it is found that hot desert (biome number 15), cool grass/shrub (14), and polar desert (17) show very good or even excellent agreement

when comparing maps of run A,B,C,D with run 30 as well as with the initial map. By contrast, for savanna (3) and xerophytic woods/shrub (11) much better agreement is found when comparing maps of run A,B,C,D and run 30 then when comparing the former with the initial map.

Concerning the differences between run A, B and run C, D, it can be inferred from Figure 4 that all biomes exhibit better agreement when comparing maps of run C, D with that of run 30 and the initial map (marked by open and full squares in Figure 4) than when comparing maps of run A, B with the latter (marked by open and full circles). This difference in agreement is particularly large for xerophytic woods/shrub (11) and savanna (3). Other biomes, particularly cold mixed forest (9), show striking differences, but these cover only a relatively small portion of the continental surface (in fact, cold mixed forest covers the smallest portion).

If the biome map computed from the average over the first five years of run A is compared with the initial map and that of run 30, the resulting κ_i (marked as “+” in Figure 4) closely resemble those from run C and run D, but disagree with those from individual years of run A. This result corroborates the following conclusion: There is a consistent difference in biome maps between run A, B and run C, D. This difference is not due to the interactive integration of climate and biome model. Otherwise, there would be a difference between run A on the one side and run B, C, D on the other side. It is obvious that the difference is caused by using single-year climatologies as in run A, B instead of multi-year climatologies as in run C, D. If a multi-year climatology is constructed from run A or B, the corresponding results are closer to that from run C, D, than from the original single-year run A and run B. The reason for this discrepancy will be discussed in Section 4.6.

4.4 Trends in biome structures

Since differences in biome structures between run A, B and run C, D, are detected, it seems worthwhile to check whether there are any differences in trends. Therefore, a trend analysis is applied to percentage land cover of each individual biome and to all κ_i , $i=1,17$, for run A, B, and C, respectively.

Concerning percentage land cover, no significant trend has been found, even not in run

C. There is only one exception: xerophytic shrub/woods significantly decrease (at 5 % significance level) in run A if all 10 years are considered. The trend becomes insignificant if the first year is omitted.

Concerning individual Kappa values κ_i , no significant trend has been found (as for global Kappa values κ), except for xerophytic woods/shrub. κ_{11} increases slightly when comparing maps of run C with the initial map. But that is the only exception.

Therefore, it can be concluded that regardless whether the combined climate-biome model or climate and biome model in an off-line mode are integrated and regardless whether the coupling of climate model with biome model is done at an interval of one or five years, there is no significant shrinking, expanding or shifting of individual biomes.

4.5 Global surface parameters

Figure 5 depicts the time series of global averages of surface parameters, leaf area index LAI , vegetation ratio c_v , forest ratio c_F , and roughness length z_{0v} , starting with the initial distribution taken as “year 0”. The full line indicates results of the climate simulation run A in which the initial biome distribution and, hence, the initial distribution of surface parameters is kept fixed, and the full line indicates just virtual changes of surface parameters. The dashed line is the result of integrations with the combined climate-biome model, run B.

From Figure 5, it is obvious that the largest change in surface parameters occurs at the first iteration, i.e. between the initial distribution and the distribution computed after the first year of integration. Surface parameters of run A and B do not exhibit any statistically significant trend, even if the initial values are included. Moreover, the hypothesis that the average of global surface parameters over the first 10 years, initial values of “year 0” excluded, differ significantly can be rejected. Not shown in Figure 5 is the background albedo which varies only little, except that the initial value is approximately $\alpha \simeq 0.18$ and the subsequent values, $\alpha \simeq 0.19$, both for off-line run A and on-line run B integrations.

The difference between surface parameters used for run A and surface parameters computed from run A in an off-line mode is rather large when comparing it with the inter-

annual variability of parameters in run B and the virtual interannual variability in run A. In other words, in the present example, the climate model tends to produce its own set of land-surface parameters regardless what is originally prescribed.

Figure 6 depicts global averages of surface parameters computed from run C (full line). Here, c_v and c_F significantly decrease (at 5% significance level), but if the initial value is disregarded, then no significant trend is left. The dotted line depicts the result of the 20-year integration run D which are close to that of run C.

When comparing surface parameters of run C and D averaged over the 20 years of integration (disregarding the initial values at “year 0”), then there are no significant differences. However, when considering the time averages of surface parameters either of run A or B and those of either run C or D, then c_v , c_F , and z_0 differ significantly at a significance level of 5%.

Obviously, incorporation of the BIOME model into the climate model ECHAM does not induce a significant trend in global averages of land surface parameters. Moreover, using the BIOME model in an off-line or on-line mode, does not alter these global averages. However, there is, again, a difference when comparing parameters evaluated from 1-year climatologies (run A and B) and multi-year climatologies (run C and D), corroborating results of Sections 4.2 and 4.3.

The global surface parameters of run A, B, C, D have to be compared with that of run 30. In run 30, the background albedo is $\alpha = 0.18$ on global average, i.e. the same global value as in the initial distribution of run A, B, C, D. Furthermore, in run 30, the leaf area index is set to a constant value of $LAI = 4$, the vegetation ratio is generally larger than in run A,B,C,D, $c_v = 0.71$ on global average, the forest ratio is smaller, $c_F = 0.27$ on global average. Also the roughness length is smaller: the overall roughness length z_0 , which includes form drag due to orography, amounts to $z_0 = 2.539\text{m}$ in run 30 which is close to $z_0 = 2.530\text{m}$, $z_0 = 2.522\text{m}$, $z_0 = 2.544\text{m}$, and $z_0 = 2.540\text{m}$ produced by run A (in an off-line mode), B, C, D, respectively; but it is much smaller than the initial value of $z_0 = 2.5902\text{m}$ used to start run A, B, C, D. On global average, the land surface parameters of run B, C, D are closer to the initial values than to that of run 30, except for the roughness length. Nevertheless, concerning the overall agreement of biome maps, it is just the other way round. Together with the above mentioned result of

virtual changes of surface parameters in run A, this indicates that globally, the influence of local changes in land surface parameters on the atmospheric general circulation is of second order in comparison to dynamical constraints such as earth's rotation or solar irradiation - provided that the ocean, or more precisely, the SST, is not changed.

4.6 Climate variables

Here, only climate variables are analysed that are used in the BIOME model, i.e. the mean temperature of the coldest month T_c , the mean temperature of the warmest month T_w , the sum of temperatures above $0^\circ C$, the sum of temperatures above $5^\circ C$, and the annual moisture availability m which is the ratio of actual and potential evaporation.

In Figure 7, global means of T_c , denoted as $\langle T_c \rangle$, are plotted versus time for run A, B, C, D. It is obvious that run A and run B reveal much smaller $\langle T_c \rangle$ than run C, D. (This difference is significant at 1% significance level.) On the other hand, there is no significant difference between $\langle T_c \rangle$ of run A and of run B when averaged over the 10-year integration period. The same is valid for run C and D. If $\langle T_c \rangle$ is computed from a 5-year or 10-year climatology of run A or B, then this $\langle T_c \rangle$ is within the standard deviation of $\langle T_c \rangle$ evaluated from run C and run D. This result could have been anticipated: extremes are reduced on average over several years, provided that these extremes occur in different months of different years.

The same argument applies to $\langle T_w \rangle$. In fact, $\langle T_w \rangle$ of run A, B are significantly (at 1% and 5% significance level, respectively) larger than of run C, D ($20.56^\circ C$ versus $20.28^\circ C$).

By contrast, the other variables do not differ significantly between run C and run B as well as between C and A. Therefore, it is justified to blame the differences in biome structures found in the previous sections on the differences in mean temperatures of the coldest and warmest month - at least from the statistical point of view.

It is hard to judge whether biome maps of run A, B or run C, D are more realistic, because this experiment is not designed to produce realistic predictions which could be validated. However, it can be stated that run C and run D yield more reasonable results for various reasons. Firstly, biome maps from run C, D agree better with the biome map from run 30 which can be considered as ECHAM's original simulation of

present-day climatology. Secondly, from the statistical point of view, the BIOME model of Prentice et al. (1992) is formulated to use climatological data. A single year does not constitute a climatology which is clearly seen when considering extreme values T_c and T_w . Thirdly, from a physical point of view, it seems more reasonable to deduce a climatological value of soil moisture availability from a multi-year climatology because the characteristic time scale of soil moisture changes is almost one year (approximately 8 months, e.g. Peixoto and Oort, 1992).

5 A drastic change in vegetation

In the first experiment, a biome distribution is initially prescribed which closely resembles today's biome distribution provided by Prentice et al. (1992) as well as the biome distribution produced by an earlier integration (called run 30) of the climate model ECHAM. As a result, the interactive and the off-line mode integrations with the climate-biome model both yield biome distributions which are similar to the initial and the run 30 biome map; in terms of Kappa statistics, they agree very well, almost excellently. These maps which are shown as Figures 9, 10, 11 (for allocation of colors to biomes, see Figure 8) are not identical because the allocation of land surface parameters to biomes has not been tuned. One of the most important results of the first experiment is that the interactive integration of climate and biome model does not enhance simulated climate variability nor induces significant trends, except for the first iteration. The first experiment is driven by moderate changes in global biome patterns; therefore, to explore whether adjustment to an equilibrium depends on the initial vegetation pattern a second experiment is designed in which the combined climate-biome model is initialized with a biome distribution which drastically differs from today's biome map.

The second experiment is set up using the experience of the first one. Climate model and biome model are not coupled at a one year interval, and the initial integration is checked for trends before the first iteration is done. The experiment is started with the same initial biome distribution of the first experiment, except that hot desert is replaced

by tropical rain forest and tropical rain forest, tropical seasonal forest, and savanna, by hot desert (see Figure 12).

With this initial vegetation distribution, the climate model is integrated for six years. Biomes and land-surface parameters are computed (in an off-line mode, of course) at the end of each year. When inspecting biome maps, there is quite some variation within the first three years. For illustration, Figure 13 depicts the interannual differences Δ and the overall agreement κ of successive years. A trend analysis reveals that only when taken the last three years of the six-year integration there is no trend in Δ for any biome, no trend in κ_i , $i=1,17$, when comparing biome maps of each year with that of run 30, and no trend in global averages of climate variables. Hence biome patterns and, consequently, land surface parameters are evaluated from the last three years of the initial integration. The resulting biome map is shown in Figure 14.

It is striking that all deserts recover at the first iteration, except for the South-West Sahara where xerophytic woods/shrub and warm grass prevail. A change from initially prescribed hot desert to the original tropical rain forest is found only in Indonesia. Obviously the dynamic constraints of the general atmospheric circulation together with the fixed SST dominate over a drastic change in land-surface conditions which is large-scale not just local, as in the first experiment. Only for the SW Sahara, summer precipitation patterns have changed over a wide area in comparison with run 30.

Using the first biome map, Figure 14, a second integration is started. To speed up computation, the second integration was done for only four years. The first out of four years is considered an initial phase to let the climate model adjust to new surface parameters. (An initial phase of one year should be sufficient, because the strongest change is expected to have occurred at the first iteration.) A climatology is computed from the last three years which is used to compute a new global distribution of biomes (shown in Figure 15) and associated land-surface parameters. This procedure is repeated for a third, fourth, and fifth 4-year integration. The biome map resulting from the last three years of the fifth 4-year integration is presented in Figure 16.

The second iteration brings the initial vegetation patterns further back to its original distribution. Rain forest and tropical seasonal forest and savanna have recovered in Latin and South America and most parts of Central Africa (see Figure 15). Differences

with the original biome distribution are still seen in the SW Sahara and in region of Ethiopia where hot desert still remains. But there are more changes which were not prescribed initially. The desert belt has stretched to the East and has invaded the Indian subcontinent. In the region around the Caspian and Aral Sea, where originally (compare with Figures 9 and 10) hot desert was simulated, now cool desert and warm grass is found. These differences do not vanish during the following iterations, see Figure 16.

Can these differences in biome patterns be traced back to changes in climate variables and, perhaps, to changes in atmospheric circulation patterns? Inspection of climate variables reveals strong differences for precipitation, cloudiness, surface soil moisture, and mean sea-level pressure (MSLP) during summer only. Other variables such as surface and atmospheric 850 hPa temperatures, 500 hPa geopotential heights show little differences throughout the seasons for all years. As one would expect, surface soil moisture and precipitation are enhanced over SW Sahara and reduced, over India. For cloudiness, the opposite is valid. These changes in the hydrological cycle are associated with changes in the general circulation patterns. As indicated by MSLP maps (See Figures 17 a, b) the Azores high pressure systems is weaker in the combined climate- biome model, and the monsoon trough over the Indian subcontinent is filled up and shifted towards Indonesia. The weakening of the Azores high pressure allows for a stronger and more far reaching intrusion of south-westerly surface winds into the Sahara, and the increase of MSLP over India characterizes the deterioration of the Indian summer monsoon. How the shift of xerophytic woods/shrubs into the SW Sahara can affect the India summer monsoon and whether this phenomenon is really consistent has to be critically reassessed by high-resolution climate models whose ability of simulating present-day climate can better be trusted than a low-resolution model used here.

The largest changes in the second experiment occur at the first and second iteration. Figure 18 and 19 illustrate this by depicting the trend of globally averaged land-surface parameters and the overall differences Δ between biome maps and global Kappa values of successive iterations, respectively. A trend analysis of differences between biome patterns in terms of percentage land cover and Kappa statistics reveals that all trends become insignificant for the last three iterations. The same is found to be valid for trends

in climate variables. Hence it seems statistically save to conclude that the combined climate-biome model has found its new equilibrium.

Sensitivities studies, not shown here, reveal that changes in albedo (within the range considered here) more strongly affect the biome patterns than changes in vegetation roughness length. Changes in leaf area index, vegetation and forest ratio have just marginal influence.

In summary of this section, after a strong perturbation of vegetation patterns it takes three iterations for the combined climate-model to approach a new equilibrium state, two more than in the first experiment. The new equilibrium differs from the original one. This indicates that some regions of the earth are more and others are less sensitive to changes in vegetation. Moreover, changes in biome patterns appear where vegetation were not altered initially.

6 Conclusion

The central purpose of this study was to explore the consequences of varying the frequency of asynchronous coupling a climate model with a biome model and to analyse the way the combined model finds its own equilibrium. To the author's knowledge, this analysis has not yet been undertaken, although this paper is not the very first one on interactive integration of a global equilibrium-response vegetation model and a atmospheric general circulation model. Here, the BIOME model of Prentice et al. (1992) and the climate model ECHAM of the Max-Planck-Institut für Meteorologie, Hamburg, have been used as biospheric and atmospheric components of the combined climate-biome model. So far, the following results have been found.

Incorporation of the BIOME model into the climate model ECHAM does not enhance the simulated variability, expressed in terms of differences between global patterns of vegetation or, equivalently, climate zones. This results corroborates Henderson-Sellers (1993) study, which is interesting because Henderson-Sellers used a different vegetation scheme and climate model. Hence this result seems to be a general one. The frequency

at which the biome and the climate model interact does not significantly alter the degree of interannual, pentadal, or decadal variability. Together with the analysis from Kappa statistics it appears that all changes occur at the first iteration, after that, apart from a minor exception, there is no significant shrinking, expanding, or shifting of biomes. Likewise, there is no significant trend found in global averages of land-surface parameters and climate variables.

It has been seen that, when started from a biome distribution which is similar to today's distribution, the combined climate-biome model finds its own new equilibrium which differs from the initial biome distribution and approaches the biome map from an earlier integration with the original version of ECHAM. On global average, land-surface parameters found during the course of interactive integration of the climate-biome model are closer to the initial distribution than to that of the original ECHAM run, except for roughness length. However, concerning overall agreement between biome maps, it is just the other way round. Since changes in albedo presumably affect local climate more strongly than changes in vegetation roughness length, it can be concluded that the atmospheric global circulation is more strongly affected by dynamical constraints than by small changes in vegetation - provided that the ocean surface temperatures are kept constant.

An interesting difference in biome maps computed from single-year and multi-year climatologies has been detected. This difference can be blamed on the statistics: extreme values used in the BIOME model, such as mean temperatures of the coldest and warmest months, are smoothed when averaged over several years. Since the BIOME model relies on long-term statistics, it is more plausible to incorporate the BIOME model into ECHAM at the end of a multi-year period, not just a single-year period. Moreover, a multi-year period is needed for the hydrological cycle to approach some equilibrium.

Starting the climate-biome model from a biome map which drastically differs from today's global distribution of biomes, it takes two more iterations until the model finds its equilibrium, which differs quite a lot from the present-day vegetation distribution in certain parts of the globe. Aforestation of the Sahara remains stable in the South-Western region of the desert, albeit the originally "planted" rain forest turns into xerophytic woods and shrub. Interestingly enough, vegetation changes from xerophytic

woods/shrub and warm grass to desert in the Indian subcontinent presumably as a consequence of a foresting of SW Sahara. It is suggested that these changes in vegetation patterns are associated with weakening of the Azores high pressure system and destroying the Indian summer monsoon. However, a detailed analysis is beyond the scope of this paper. Further investigation with a high-resolution climate model and integration over longer periods are needed to decide whether this phenomenon is consistent and significant. Only then it will be save to conclude whether these changes are directly induced by alteration of vegetation, or whether vegetation changes serve as “the beat of a butterfly’s wing” to push climate into a different mode. The present analysis is just a study of more technical aspects. It will be continued to explore the possibility of other stable climate-vegetation equilibria given the present-day SST field.

To predict realistic global vegetation and climate, the climate-biome model has to be optimized. This has not yet been done, because there are several problems. Allocation of land-surface parameters to biomes is more or less a first, although educated and not unrealistic guess. It does not seem to be a bad guess because the climate-biome model yield very good, for some biomes even excellent agreement with the original version of the climate model. Nevertheless, the allocation could be tuned to yield even better agreement.

Before aiming at a realistic prediction of present-day climate with the climate-biome model, an agricultural component of global vegetation has to be introduced. After all, man has modified almost 20% of the earth’s surface. An attempt to include an agricultural component in the BIOME model has been made by Cramer and Solomon (1993). The new version of the climate model ECHAM (level 4) will use land-surface parameters which are deduced from Olson’s et al. (1982) map of major ecosystems, including ecosystems strongly affected by man. Hence, the new version of ECHAM will be more suitable as atmospheric component of a combined climate-biome model.

An important aspect of climate variability has been left out of this study: the dynamics of ocean circulation. Up to now, studies of the effect of vegetation changes on climate have been done with an atmospheric circulation model coupled with, at best, an oceanic mixed layer model in which the meridional oceanic heat transport is just parameterized. Work in progress with a coupled global atmosphere-ocean model (Latif, Hoffmann,

Claussen, Max-Planck-Institut für Meteorology) suggests that deforestation of tropical rain forest induces an increase of sea-surface temperatures in the tropical Western and Eastern Pacific as well as in the tropical Atlantic. Hence it has to be expected that a coupled atmosphere-biosphere-ocean general circulation model (ABOGCM) will exhibit an enhanced variability and will, presumably, adopt equilibrium states which differ from a climate-biome model with fixed ocean temperatures. It is hoped that this study provides guidance in constructing a ABOGCM.

Acknowledgements

The author would like to thank Colin Prentice, Dept. of Plant Ecology, Lund University, Sweden, for making the biome model available. Thanks are also due to Uwe Schulzweida and Monika Esch, Max-Planck-Institut für Meteorologie, Hamburg, for programming assistance. The author appreciates helpful suggestions by Lennart Bengtsson and Martin Heimann, Max-Planck-Institut für Meteorologie.

References

- Baumgartner A, Mayer H and Metz W (1977) Weltweite Verteilung des Rauigkeitsparameters z_0 mit Anwendung auf die Energiedissipation an der Erdoberfläche. *Meteorolog.Rdsch.* 30: 43-48.
- Claussen M (1991) Estimation of areally-averaged surface fluxes. *Boundary-Layer Meteorol.* 54: 387-410
- Claussen M (1993) Shift of biome patterns due to simulated climate variability and climate change. *Climate Dyn.*, submitted, also available as Report 115, Max-Planck-Institut für Meteorologie, Hamburg, F.R.G.
- Claussen M and Esch M (1994) Biomes computed from simulated climatologies. *Climate Dyn.* 9: 235-243.
- Claussen M, Lohmann U, Roeckner E, Schulzweida U (1994): A global data set of land-surface parameters. Report (in press) Max-Planck-Institut für Meteorologie, Hamburg, F.R.G.
- Cramer WP, Solomon AM (1993) Climatic classification and future global redistribution of agricultural land. *Clim. Res.* 3: 97-110.
- Cubasch U, Hasselmann K, Höck H, Maier-Reimer E, Mikolajewicz U, Santer BD, Sausen, R (1992) Time -dependent greenhouse warming computations with a coupled ocean-atmosphere model. *Climate Dyn.* 8: 55-69.
- FAO/UNESCO (1974) Soil map of the world 1:5,000,000. FAO, Paris.
- Geleyn J-F and Preuss HJ (1983) A new dataset of satellite-derived surface albedo values for operational use at ECMWF. *Arch.Meteor.Geophys.Biocl.*, Ser.A 32: 353-359.
- Henderson-Sellers A (1993) Continental vegetation as a dynamic component of global climate model: a preliminary assessment. *Climatic Change* 23: 337-378
- Heise E, Jacobs W, Ketterer M, Renner V (1988) Klimasimulation mit atmosphärischen Modellen im Zeitskalenbereich von Monaten. Abschlußbericht des BMFT-Projektes KF 2012 8, Deutscher Wetterdienst, Offenbach.

- Henderson-Sellers A, Wilson MF, Thomas G, Dickinson RE (1986) Current global land-surface data sets for use in climate-related studies. NCAR Technical Note NCAR/TN-272+STR, National Center for Atmospheric Research, Boulder, Colorado.
- Leemans R and Cramer W (1991) The IIASA database for mean monthly values of temperature, precipitation, and cloudiness on a global terrestrial grid. IIASA Research Report RR-91-18, Laxenburg, Austria.
- Martin P (1993) Vegetation responses and feedbacks to climate: a review of models and processes. *Climate Dyn.* 8: 201-210.
- Matthews E (1984) Vegetation, land-use and seasonal albedo data sets: documentation of archived data tape. NASA Technical Memorandum 86107, Goddard Space Flight Center, New York.
- Mintz Y (1984) The sensitivity of numerically simulated climates to land-surface boundary conditions. in: Houghton J *The global climate*. Cambridge Univ. Press.
- Monserud RA, Leemans R (1992) Comparing global vegetation maps with Kappa statistic. *Ecological Modelling* 62: 275-293.
- Monserud RA, Tchebakova NM, Leemans R (1993) Global vegetation change predicted by the modified Budyko model. *Climatic Change* 25: 59-83.
- Olson JS, Watts JA, Allison LJ (1983) Carbon in live vegetation of major world ecosystems. ORNL-5862, Oak Ridge National Laboratory, Oak Ridge.
- Peixoto JP, Oort AH (1992) *Physics of Climate*. American Institute of Physics, New York.
- Perlwitz J (1992) Preliminary results of a global SST anomaly experiment with a T42 GCM. *Annales Geophysicae Abstracts of the VII General Assembly of the European Geophysical Society in Edinburgh, Apr. 6-10, 1992*.
- Prentice IC, Cramer W, Harrison SP, Leemans R, Monserud RA, and Solomon AM (1992) A global biome model based on plant physiology and dominance, soil properties and climate. *Journal of Biogeography* 19: 117-134.
- Prentice KC, Fung IZ (1990) The sensitivity of terrestrial carbon storage to climate change. *Nature* 346: 48-51.

Roeckner E, Arpe K, Bengtsson L, Brinkop S, Dümenil L, Kirk E, Lunkeit F, Esch M, Ponater M, Rockel B, Sausen R, Schlese U, Schubert S, Windelband M (1992) Simulation of the present-day climate with the ECHAM model: Impact of model physics and resolution. Report 93, Max-Planck-Institut für Meteorologie, Hamburg.

Tibaldi S and Geleyn J-F (1981) The production of a new orography, land-sea mask and associated climatological surface fields for operational purposes. ECMWF Tech.Memo. 40.

Wilson MF and Henderson-Sellers A (1985) A global archive of land cover and soils data for use in general circulation climate models. *Journal of Climatology* 5: 119-143.

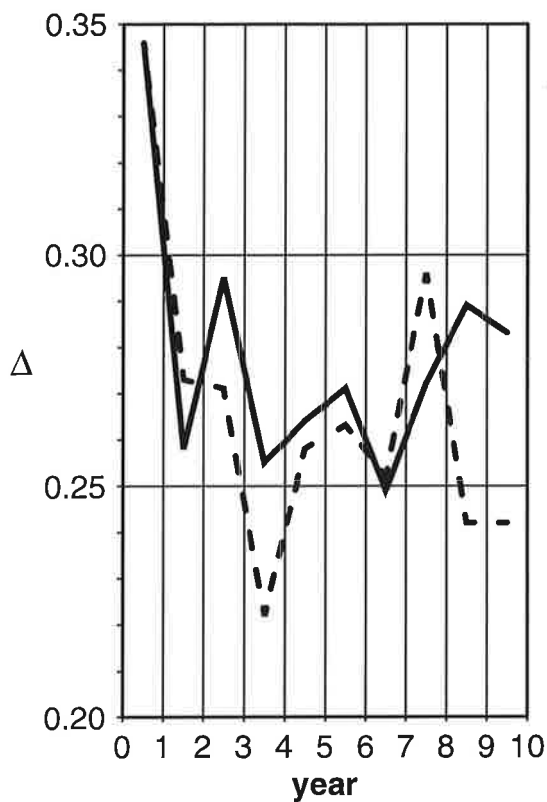


Figure 1: Interannual changes in the predicted percentages of continental vegetation, Antarctica excluded, for run A (full line) in which climate and biome model operate separately (in an off-line mode) and for run B (dashed line) of the combined climate-biome model. “Year 0” is used for the initial biome distribution. For definition of Δ , see Section 4.1.

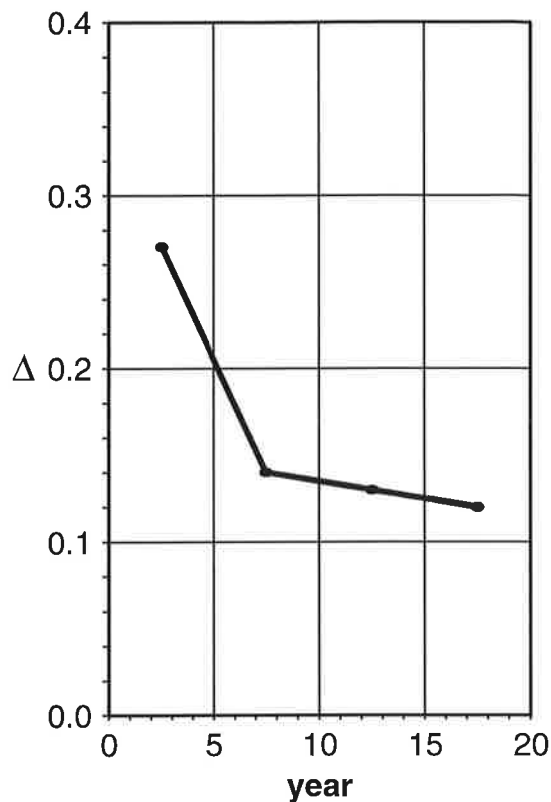


Figure 2: Same as Figure 1, except for pentadal changes in run C in which climate and biome model interfere at a 5-year period.

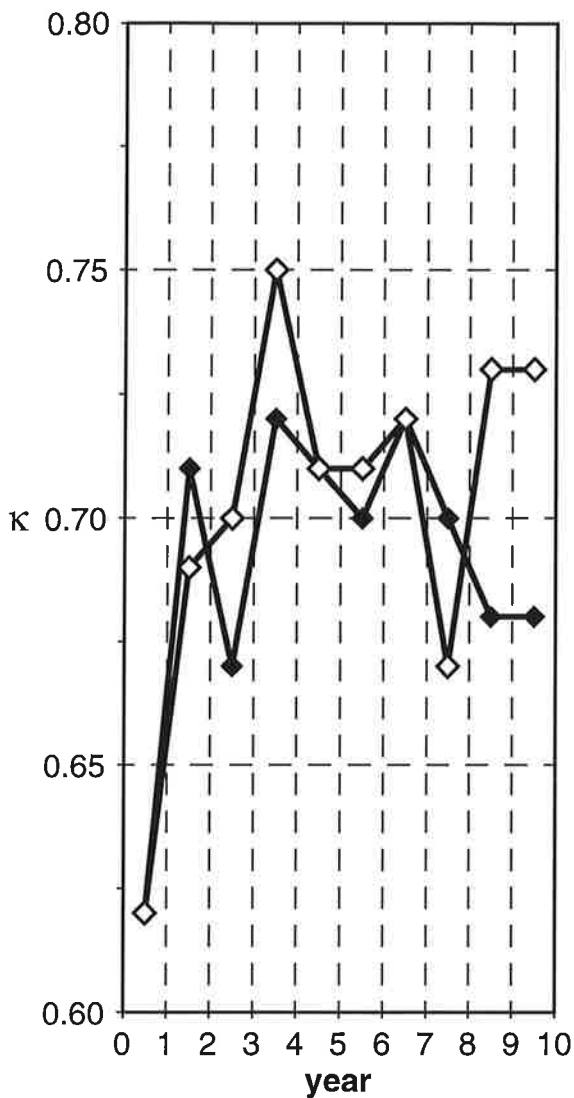


Figure 3a: Global agreement of biome maps from successive years of run A (full diamonds) and run B (open diamonds). For allocation of Kappa values to a subjective scale see text.

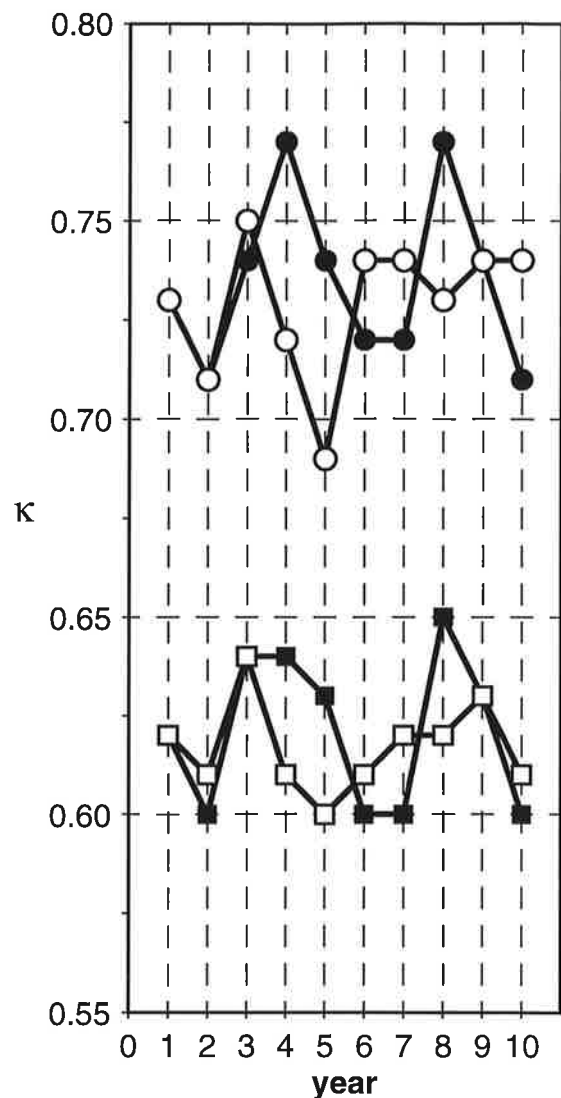


Figure 3b: Global agreement of biome maps of run A (full squares) and run B (open squares) with the initial biome map. Full and open circles indicate agreement of biome maps of run A and run B, respectively, with the biome distribution from an earlier integration, called run 30 in the text.

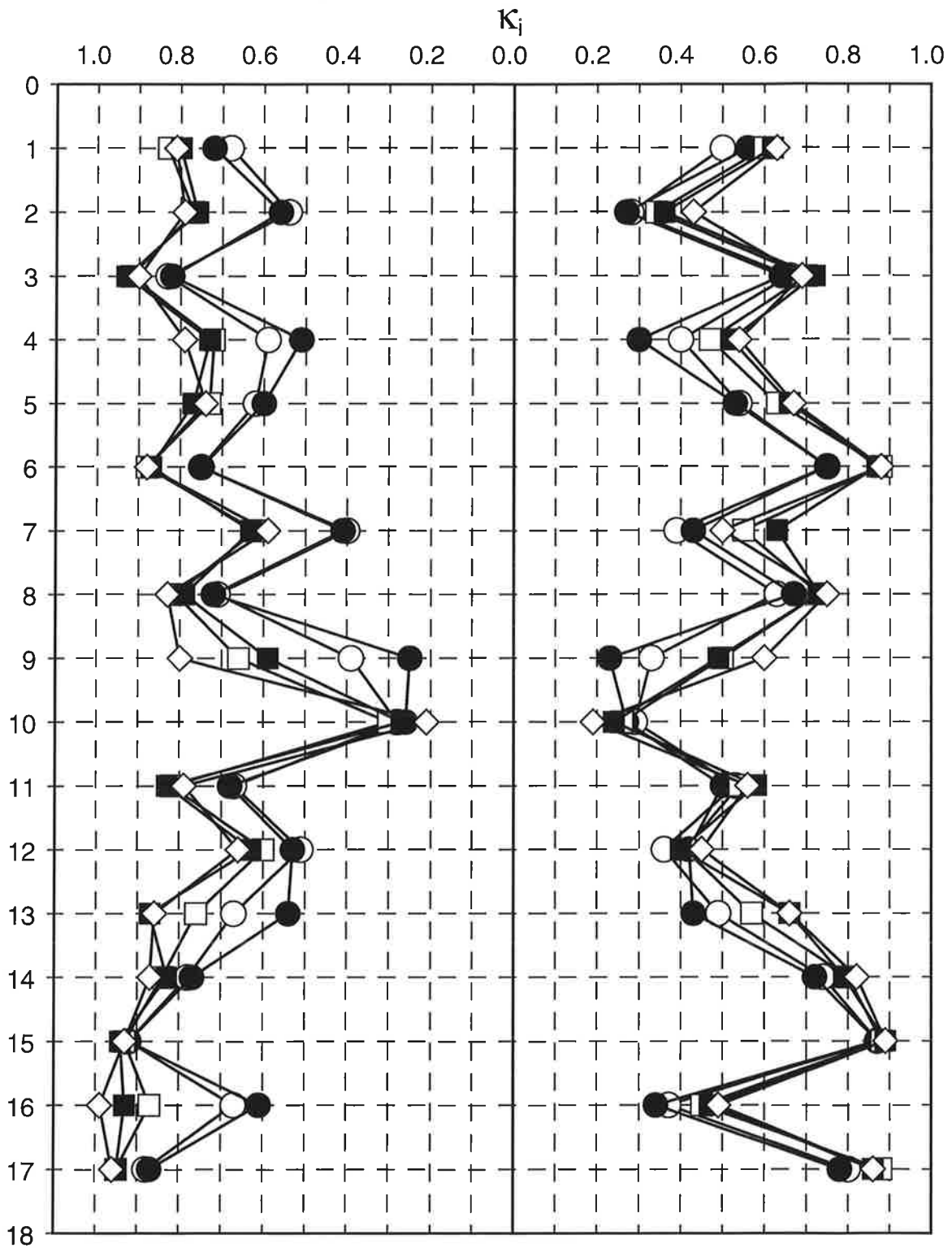


Figure 4: Agreement of individual biomes from maps of run A, B, C, D with that of run 30 (left hand side) and with the initial biome map (right hand side). Symbols indicate run A (open circles), run B (full circles), run C (open squares), run D (full squares), and a 5-year average from run A (open diamonds).

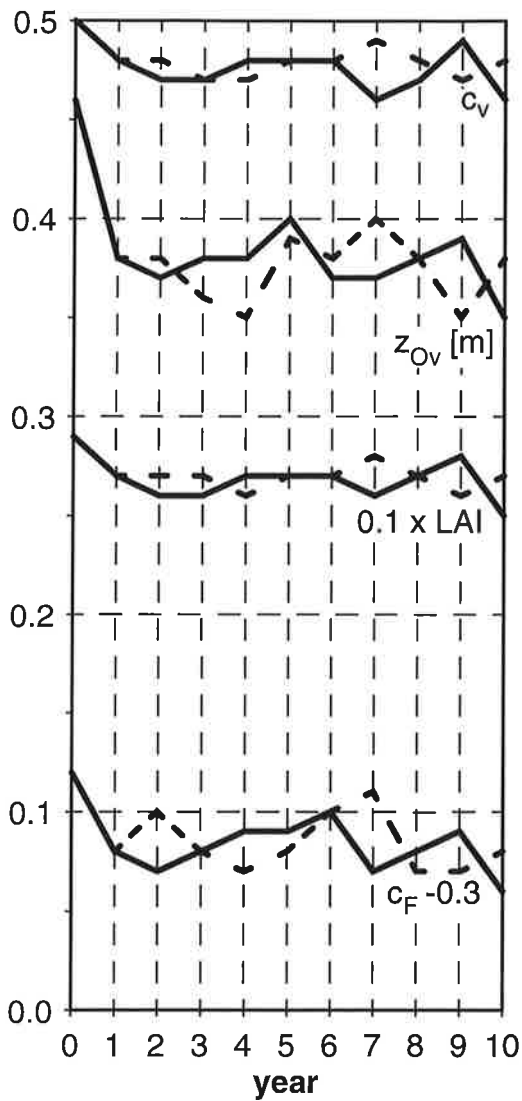


Figure 5: Global averages of land-surface parameters, vegetation ratio c_v , vegetation roughness length z_{Ov} , leaf area index LAI , and forest ratio c_F , as function of time. Full line refers to virtual changes in run A, dashed line, to changes in run B.

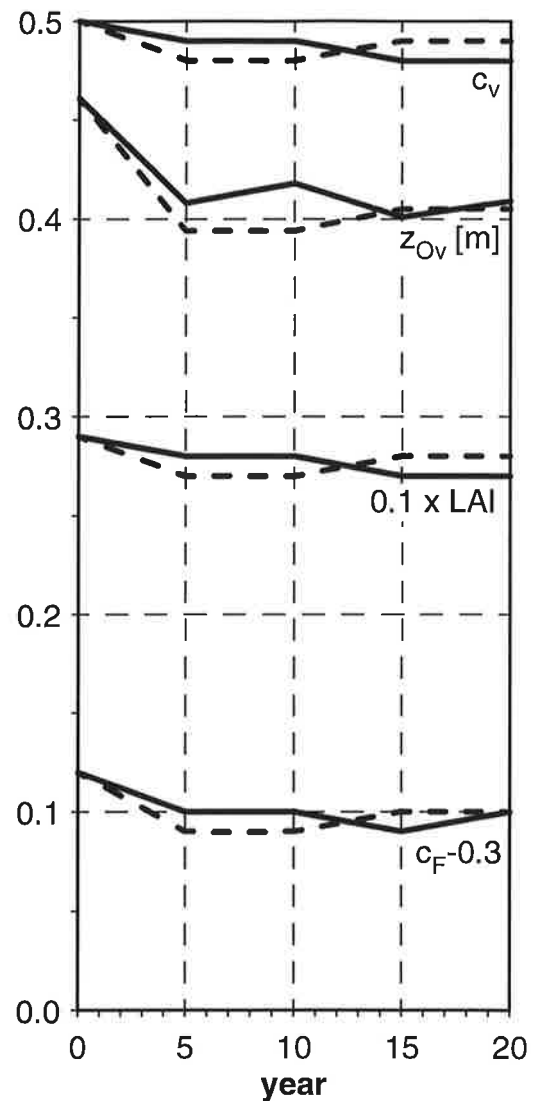


Figure 6: Same as Figure 5, except for run C (full line) and run D (dashed line).

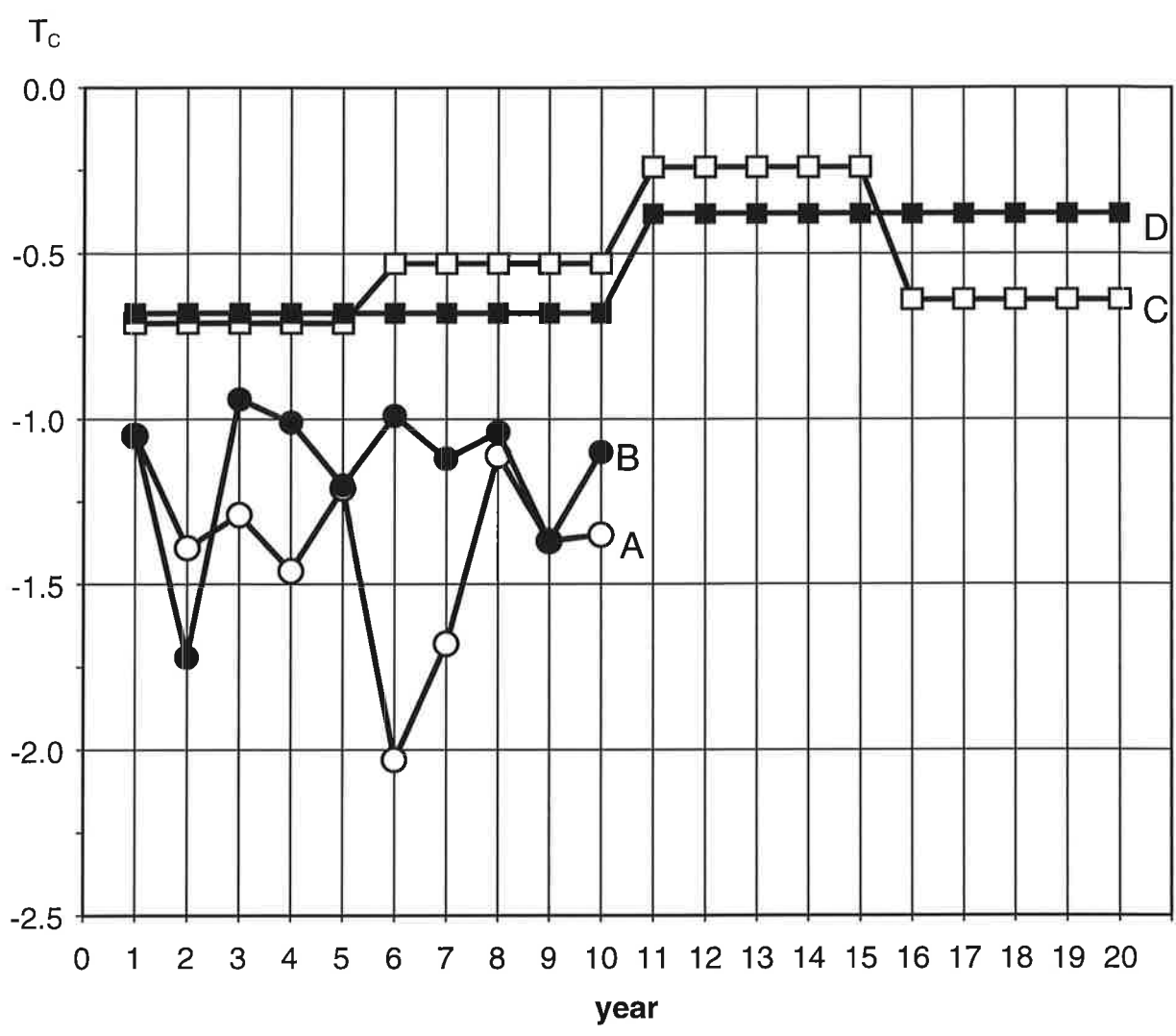


Figure 7: Mean temperature of the coldest months as function of integration time in run A (open circles), run B (full circles), run C (open squares), and run D (full squares).

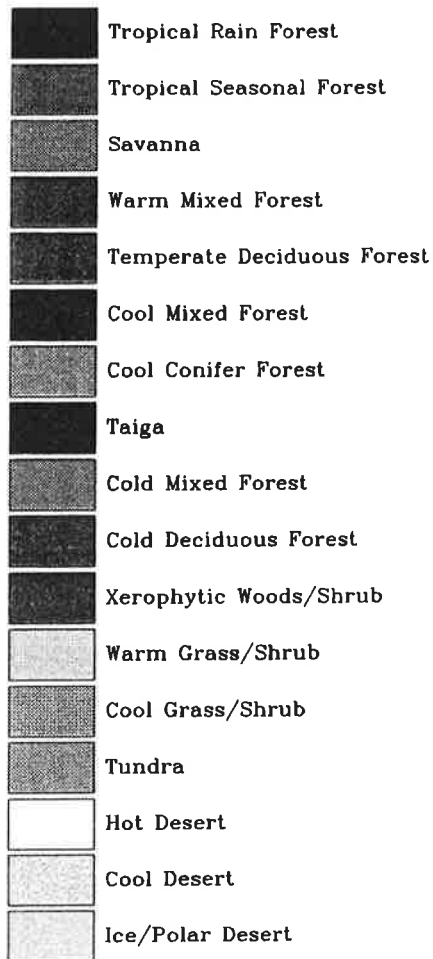


Figure 8: Allocation of colors used in Figures 9-12 and 14-16 to biomes.

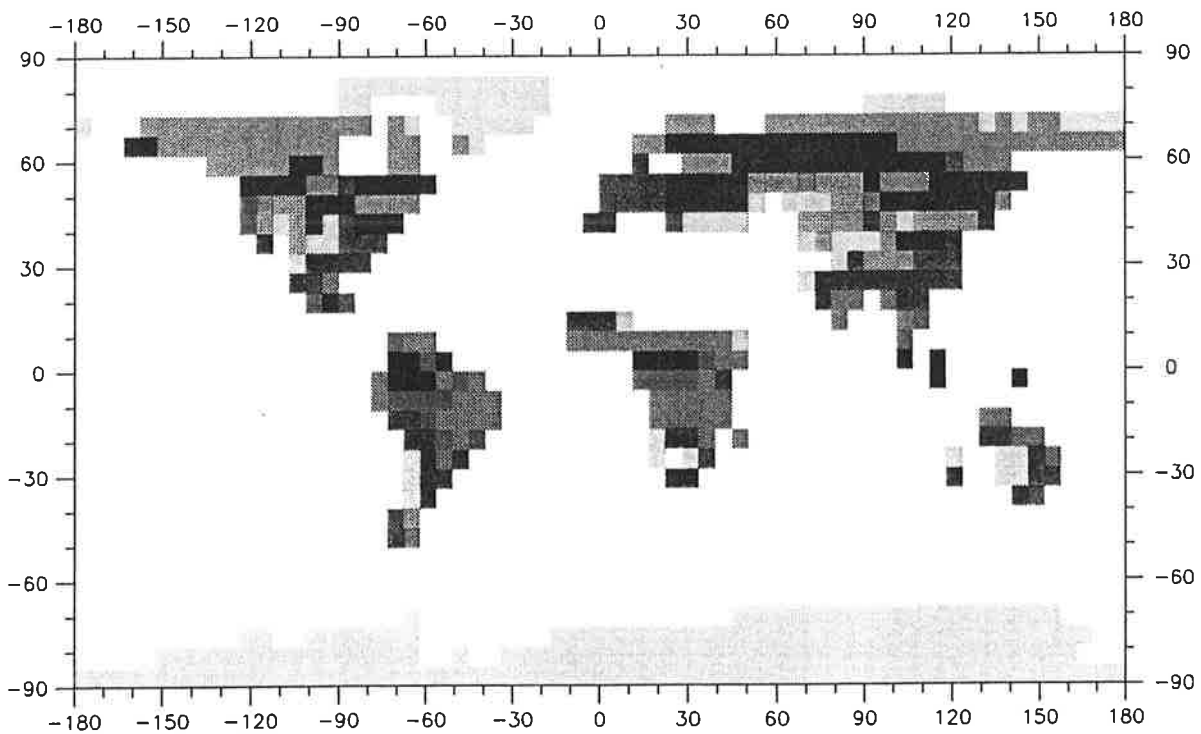


Figure 9: Initial biome distribution of run A, B, C, D.

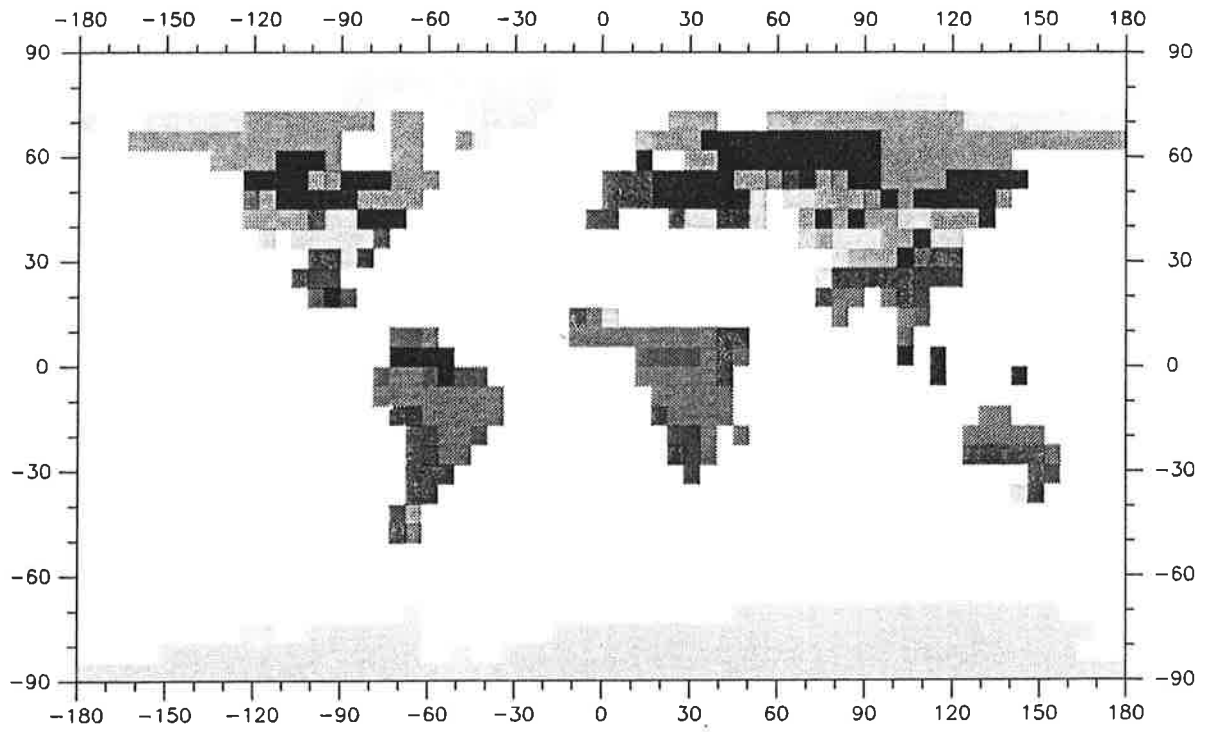


Figure 10: Biome distribution computed from the second 10-year integration period of run D.

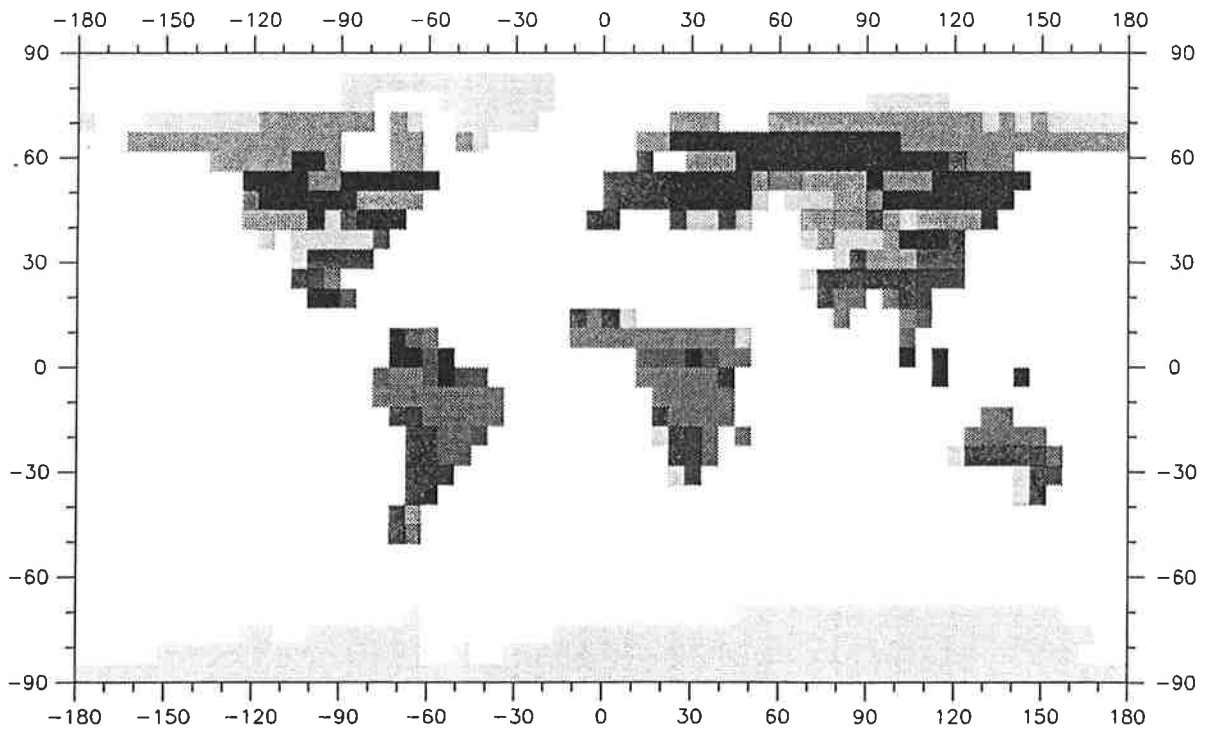


Figure 11: Biome distribution from an earlier 30-year integration with the original version of the climate model ECHAM3, called run 30 in the text.

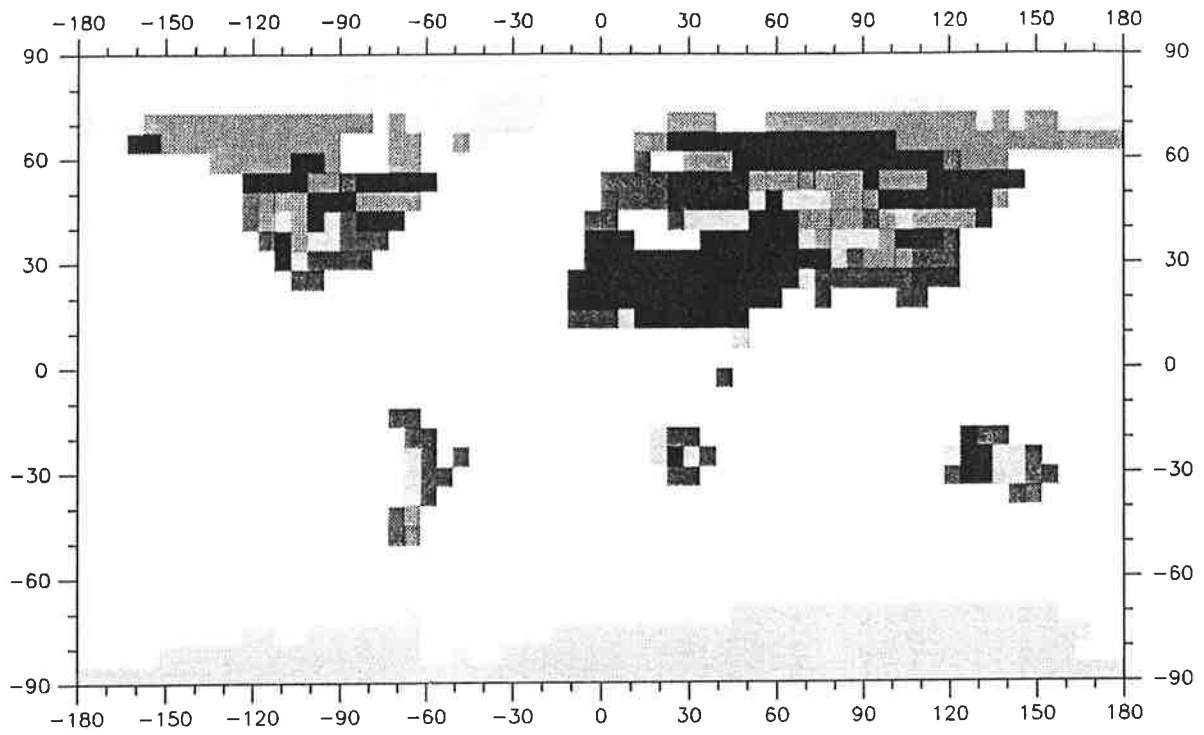


Figure 12: Initial biome distribution of the second experiment.

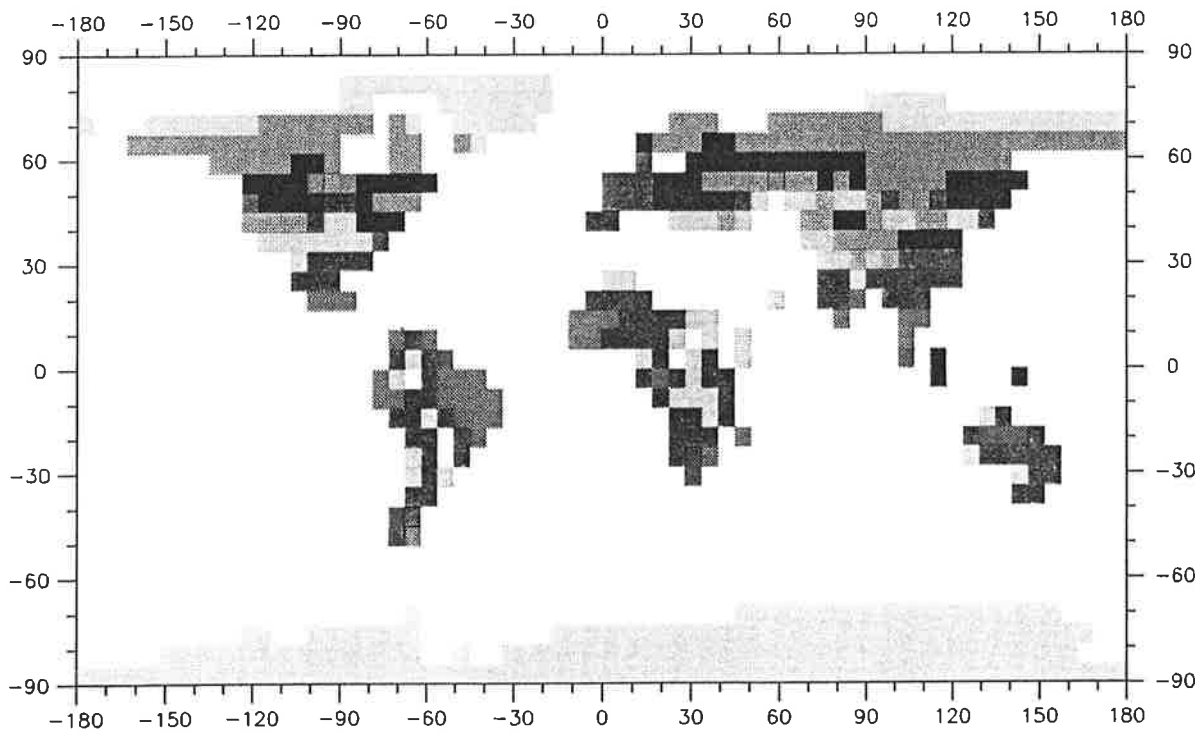


Figure 14: Biome distribution computed from an average over years 4 to 6 of the initial integration period of the second experiment.

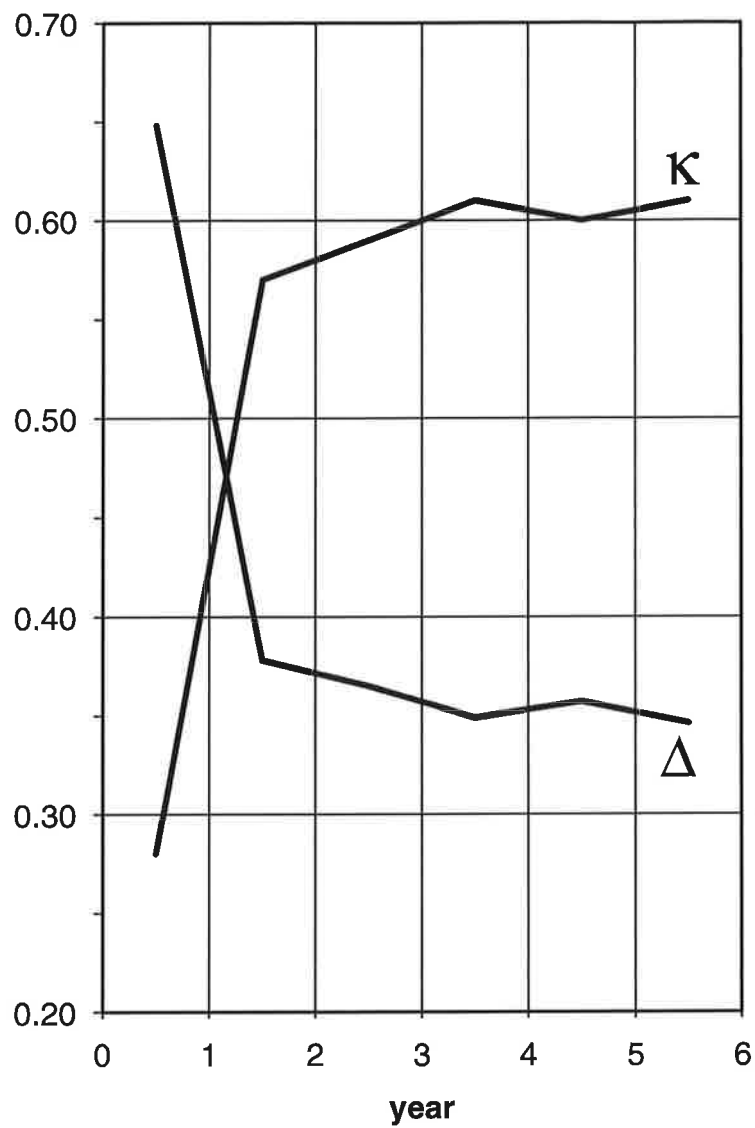


Figure 13: Difference Δ in biome maps (for Definition of Δ , see Section 4.1) and global agreement κ (see Section 4.2) between the initial six successive years of the second experiment.

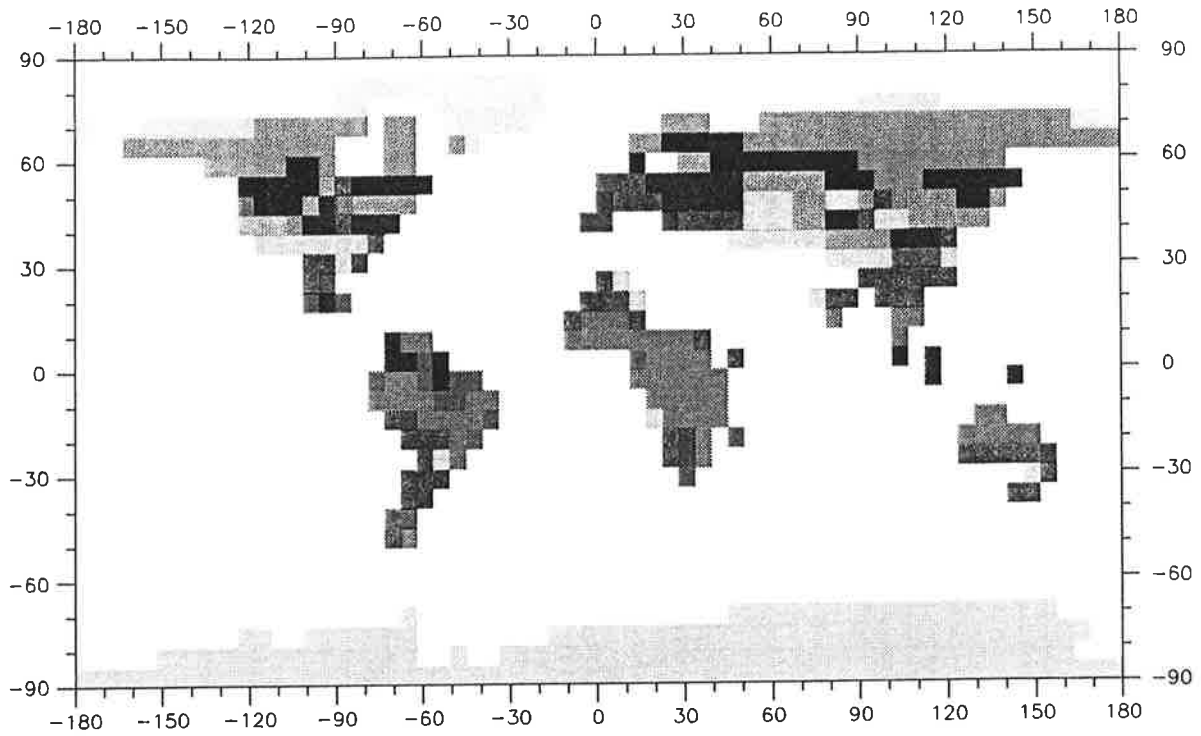


Figure 15: Same as Figure 14, except for years 7 to 8, i.e. the last three years of the second integration period.

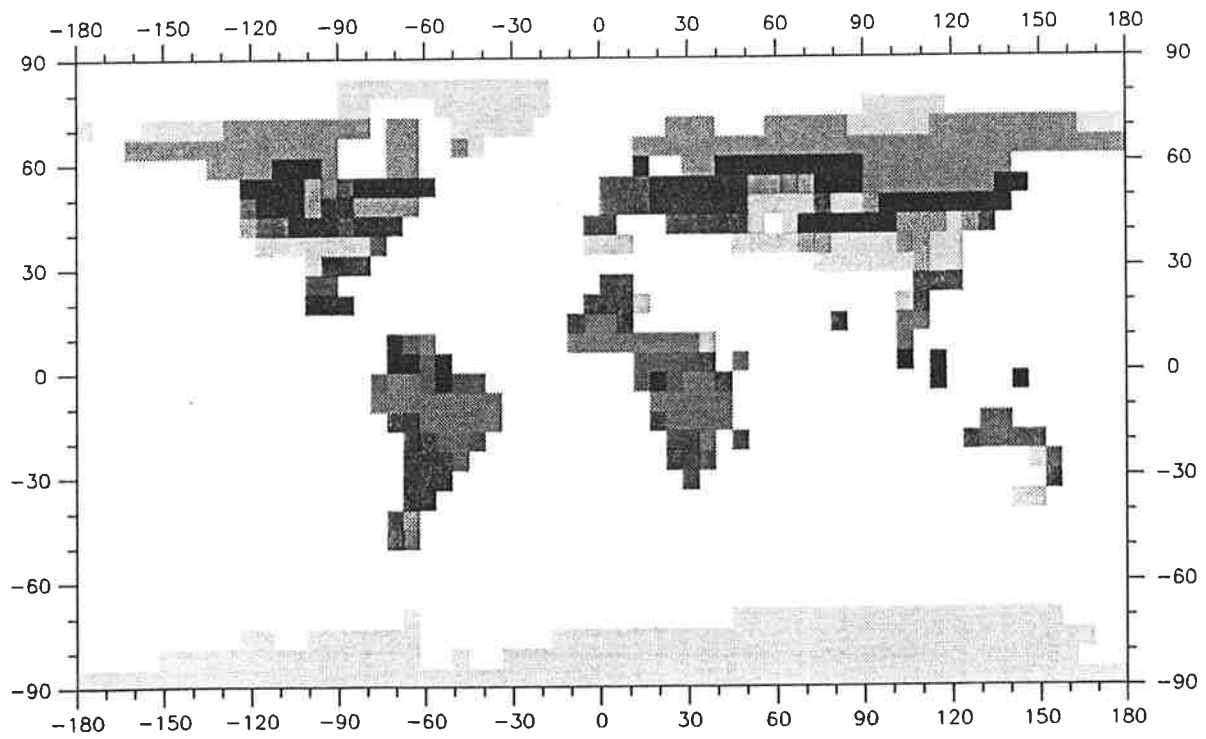
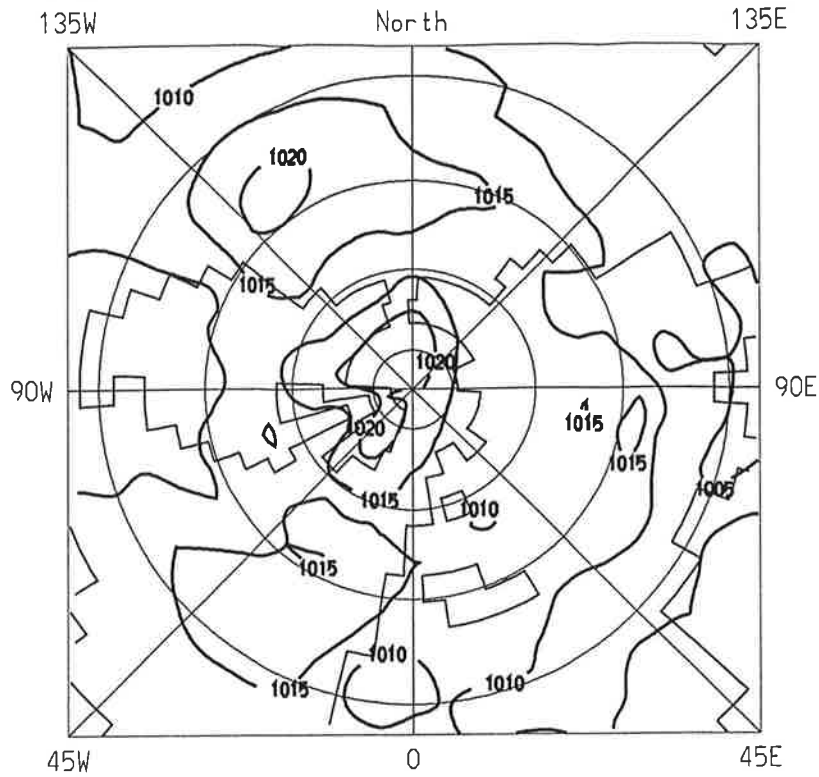


Figure 16: Same as Figure 14, except for years 20 to 22, i.e. the last three years of the fifth and last integration period.

a)



b)

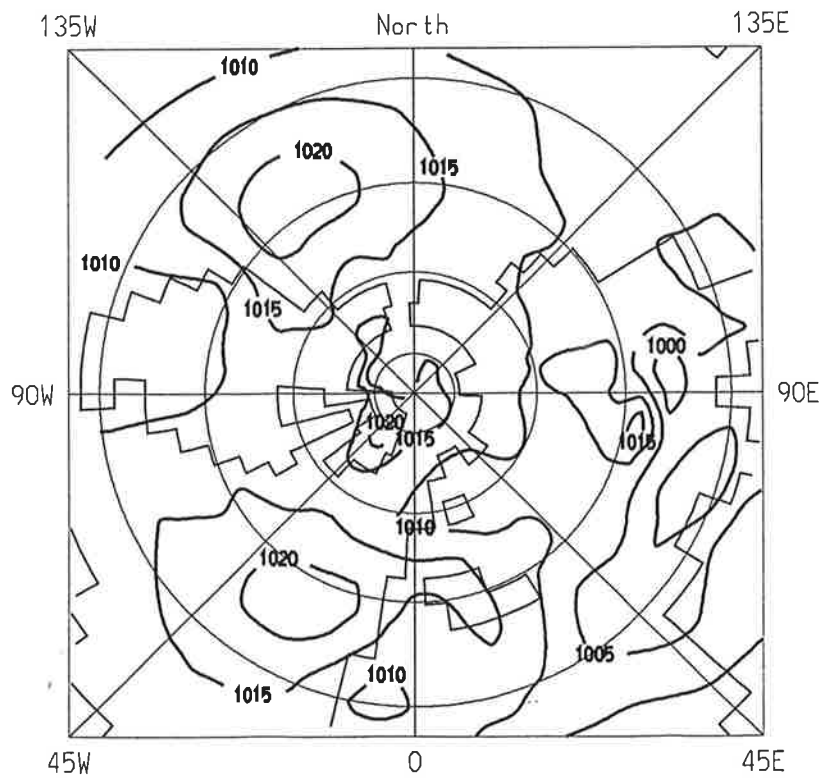


Figure 17: Northern hemisphere mean sea-level pressure (hPa) in July on average over three years of the second experiment (a) and the first ten years of run 30 (b).

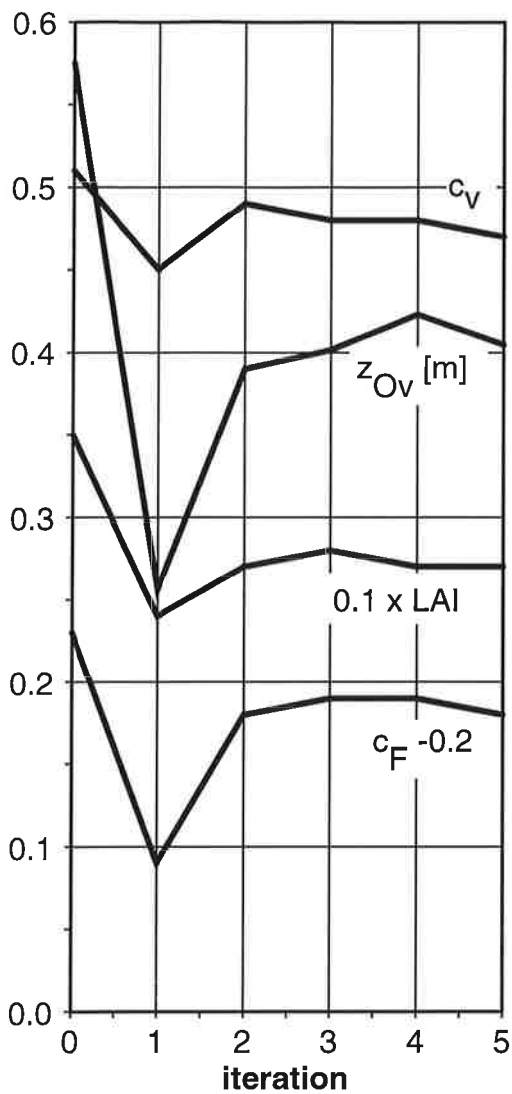


Figure 18: Global averages of land-surface parameters, vegetation ratio c_v , vegetation roughness length z_{Ov} , leaf area index LAI , and forest ratio c_F , computed from the last three years of each integration period of the second experiment. “Year 0” refers to the initial distribution of land-surface parameters.

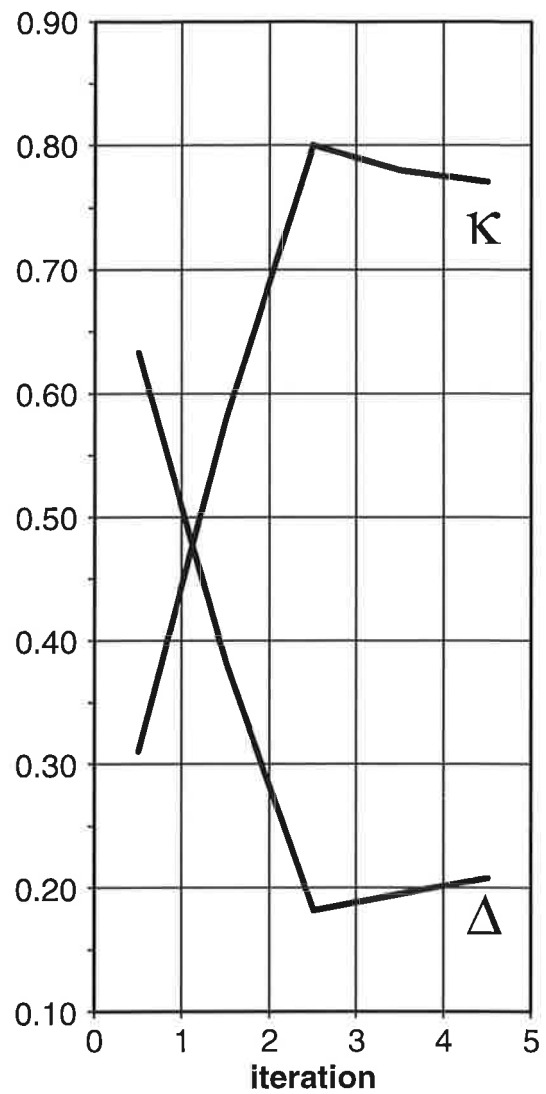


Figure 19: Difference Δ in biome maps and global agreement κ between successive iterations of the second experiment.